Numerical Simulation of Katabatic Wind Profile at Syowa Station, Antarctica

Takashi ADACHI*

南極昭和基地て観測された斜面下降風の鉛直分布の数値シミュレーション

安 達 隆 史*

要旨 南極昭和基地て観測されたレーウィンゾンテのテータのうちて典型的なカタバティック風てあると思われる 8 m/s 以上の強風を選んて解析し，風向風速と気温の鉛直分布の特徴を調査したところ，高さが 200～300 m の層て風速および気温が最大になることがわかり，さらにウィント・スパイラルが左まわりになっていることがわかった.

そして大気の安定度や温度風と斜面の効果を考慮し，さらに定常て斜面に沿った 2 次元の一様流を仮定した時に成立する運動方程式系を数値計算によって解いたところ，風速の鉛直分布とウィンド・スパイラルのパターンが実測テータと一致する解を得ることかてきた

たたし，この運動方程式系を導入する際には次のような仮定を用いた.

すなわち，接地気層て用いられた Monin-Obukhov の相似則をエクマン層全体に拡張する．たたしエクマン層の各高さにおける熱と運動量のフラックスを用いて Monin-Obukhov の長さ (L) は定義されるとし，無次元化風速シャー関数 (ϕ) については中立または安定状態て次式を仮定した.

$$\phi=(1+12z/L)^{1/2}$$

***Abstract*:** The vertical profiles of the strong katabatic winds at Syowa Station, Antarctica, are studied. A numerical solution of the equations of the Ekman layer above the Antarctic coastal slope is obtained under the following assumptions,

(a) The steady state condition

(b) The wind component of normal direction to the sloped plane is zero

(c) The wind vectors are uniform along the slope at each height

(d) Monin-Obukhov's similarity theory is valid in each thin layer of Ekman layer

(e) Local value of Monin-Obukhov length is defined by the local heat flux and the local momentum flux

(f) New non-dimensional wind shear function (ϕ) is presented in neutral or stable Ekman layer,

$$\phi=(1+12\,z/L)^{1/2}$$

* 日本気象協会・研究所 Research Institute of Japan Weather Association, Kaiji Center Bldg, 5, Koji-machi 4-chome, Chiyoda-ku, Tokyo 102

where,

ϕ : Non-dimensional wind shear function which is defined by the local shear stress and the local wind shear,

L : Local value of Monin-Obukhov length,

z : Height.

It is shown that the results of the numerical simulation of the strong katabatic wind profile agree well with the observed strong katabatic wind profiles at Syowa Station.

1. Introduction

It is well known that the katabatic winds are the winds blowing down along the ice slope on the Antarctic coast or the ice caps of Greenland.

The katabatic winds on the Antarctic coastal slope were studied by several researchers. For example, BALL (1956, 1960) studied and presented a simple theory on the strong katabatic winds. MORITA (1968) reported some characteristics of the observed surface winds at Syowa Station. ADACHI (1974) found that the power spectra of vertical wind fluctuations and air temperature fluctuations, observed at Syowa Station, have some local peaks in a relatively lower frequency range, which corresponded to the periods of 1–2 minutes. The local peaks of the spectra seem to be due to the katabatic motions or the gravity waves.

KOBAYASHI (1978) reported the observational results and investigated the vertical structure of katabatic winds in the Mizuho Plateau. The Mizuho Plateau is an inland 270 km away from Syowa Station. The Ongul Straight, which has a width of 5 km, exists between Syowa Station and the Antarctic coast. Therefore, it seems that the characteristics of the katabatic winds on the Mizuho Plateau are different from those at Syowa Station.

LETTAU (1966) studied the theoretical profiles of wind and air temperature at Amundsen-Scott Station on the gently sloping central Antarctic Plateau. The gradient of this slope is 1.76 ± 0.26 m/km. According to SHIMIZU *et al.* (1978), the Antarctic coastal slope near Syowa Station is 41×10^{-3} in the area lower than 500 m, and 14×10^{-3} between 500 m and 1000 m. Therefore, it seems that the characteristics of the winds at Amundsen-Scott Station are different from those at Syowa Station.

LYKOSOV and GUTMAN (1972) obtained the numerical solution of the turbulent boundary layer above a sloping underlying surface. However, it seems that the comparative study of the observed results with the calculated results is not enough in their report.

It is the purpose of this paper to present the characteristics of the strong katabatic wind profiles at Syowa Station and the numerical simulation of the strong katabatic wind profiles.

2. Observed Data

The aerological data of Rawinsonde in 1969–1971 at Syowa Station are used in this analysis. The selection conditions of the data are as follows;

(a) 03 local time data

(b) Clear sky condition; Total cloud amount is equal to or less than 1.

(c) Strong wind condition; Surface wind velocity is equal to or larger than 8 m/s.

The selected wind and temperature data are grouped for each month. First, the observed wind direction and wind speed are converted to North-South wind component and East-West wind component. Next, the vertical profiles of two wind components are averaged on every month data. Then, the averaged every month data are again converted to wind direction and wind speed.

Fig. 1 shows the vertical profiles of two wind components in January Fig. 2 a shows the vertical profile of the averaged wind speed in January. Fig. 2c shows the averaged wind spiral in January

Temperature differences from surface air temperature are averaged for every month (see Fig 2b)

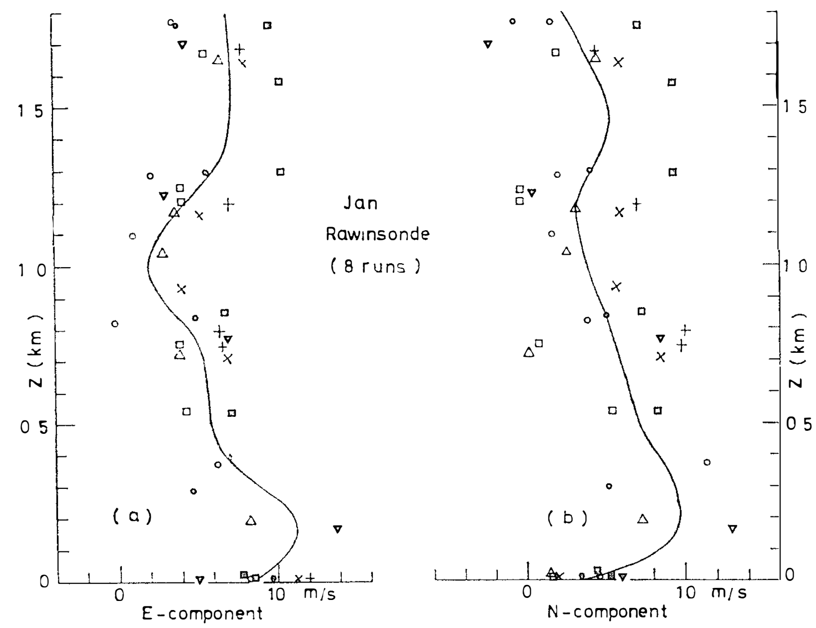

Fig 1 The vertical profiles of the averaged wind components in January.

a E–W component of wind speed

b· N–S component of wind speed

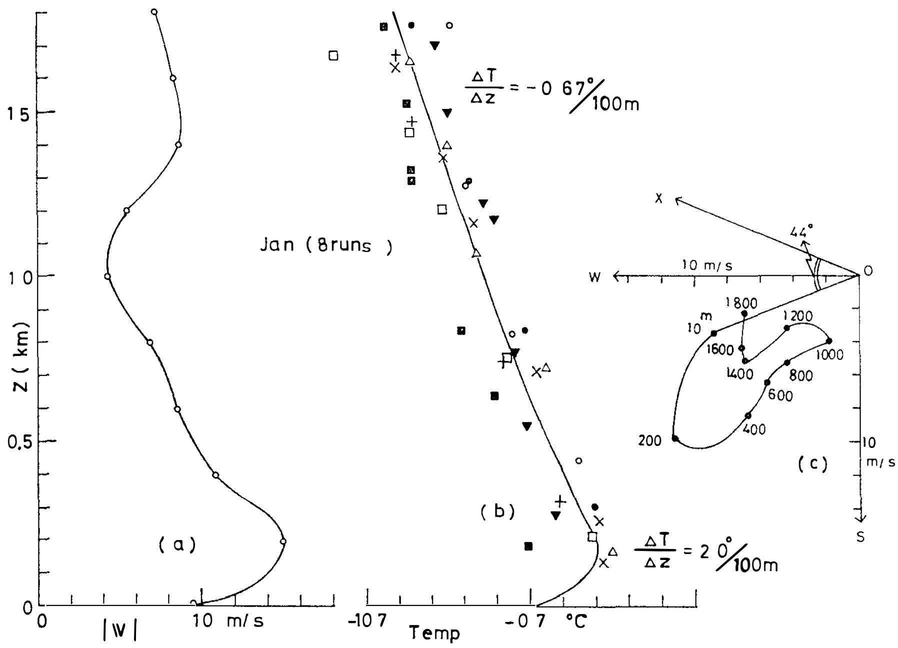

Fig. 2. Observed vertical profiles of wind speed (a) and temperature (b), and observed wind spiral (c) in January.

Characteristics of wind speed profiles and wind spirals are that the height of maximum wind speed is about 200 m and the wind spirals are counterclockwise (see Figs. 2–5). Characteristics of temperature profiles are shown in Fig. 6. The temperature

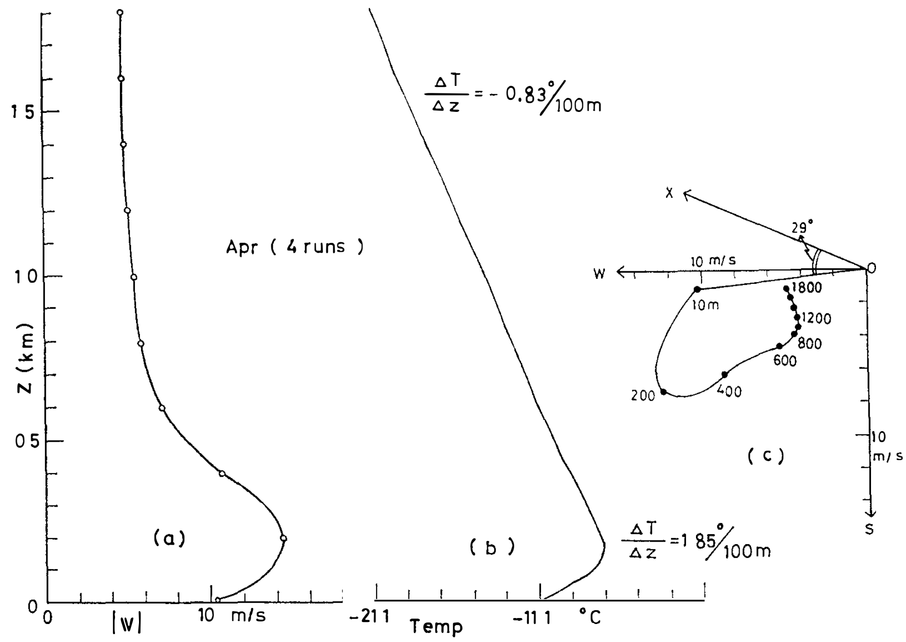

Fig. 3. Observed vertical profiles of wind speed (a) and temperature (b), and observed wind spiral (c) in April.

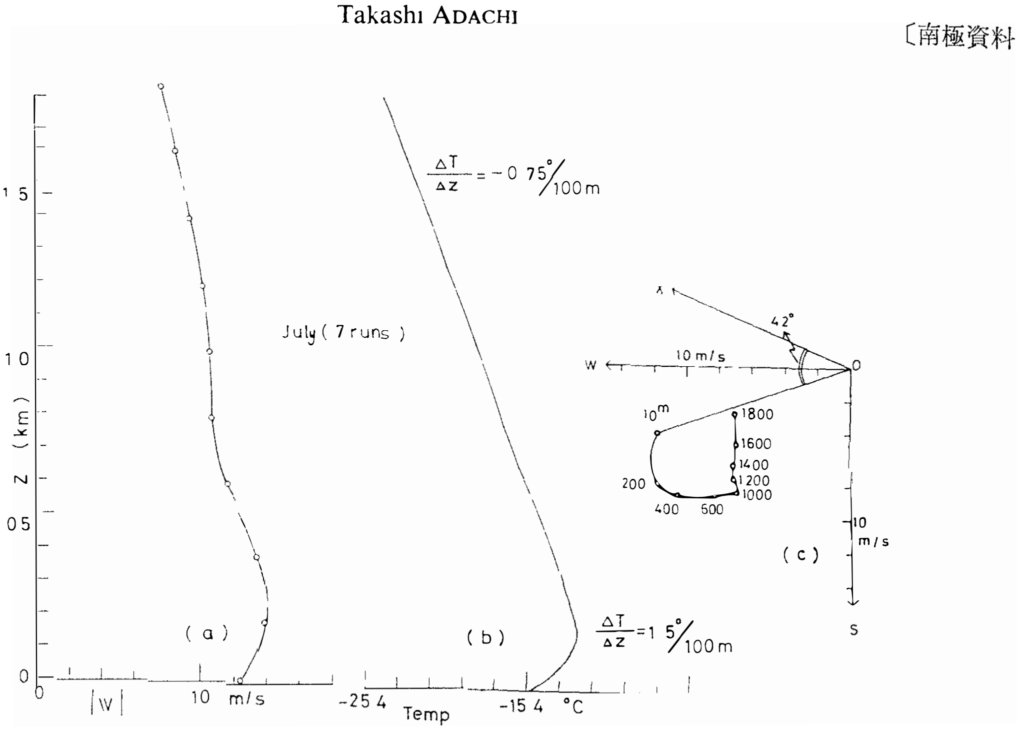

Fig. 4 Observed vertical profiles of wind speed (a) and temperature (b), and observed wind spiral (c) in July

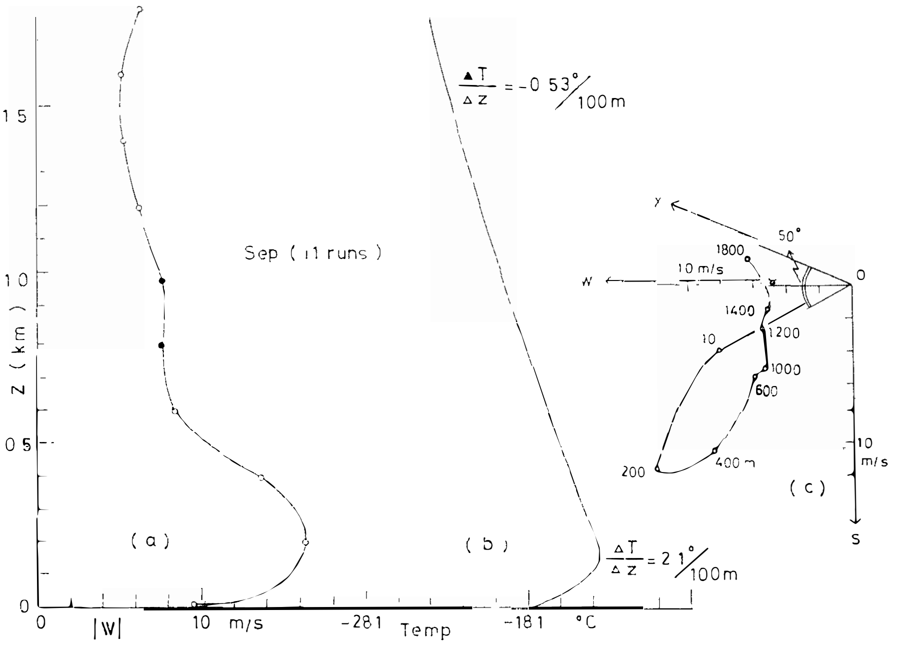

Fig. 5 Observed vertical profiles of wind speed (a) and temperature (b), and observed wind spiral (c) in September

gradient between the surface and the 200 m height is about 1.8°C/100 m. The temperature gradient between the heights of 1.2 km and 1.8 km is about −0.7°C/100 m

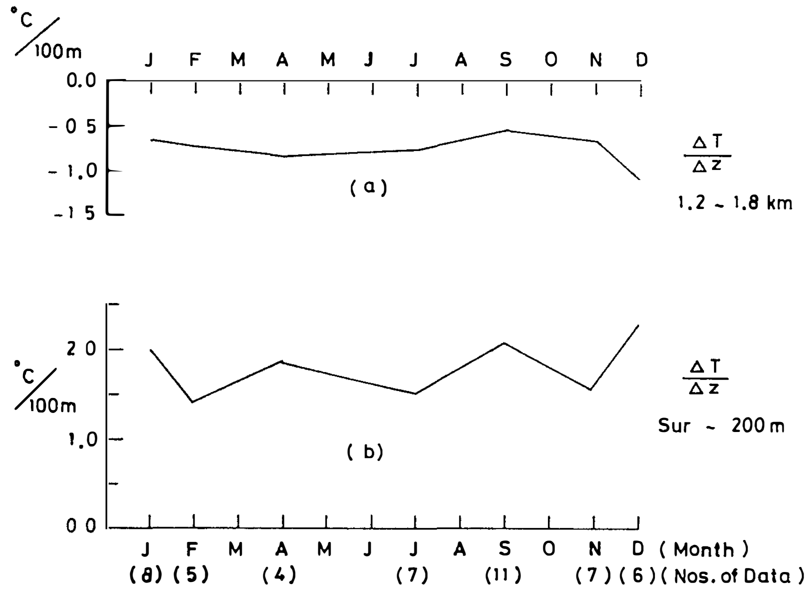

Fig 6 Temperature gradiants between 1 2 km and 1 8 km heights (a) and between surface and 200 m height (b)

3. Model of the Numerical Simulation of Katabatic Wind

3.1. Governing equations

The governing equations of Ekman layer are non-linear differential ones. Effects of the stabilities, the baroclinisities and the slope are taken into consideration in this model. The coordinates system is illustrated in Fig. 7.

The present assumptions are as follows;

(a) The stationary condition.

(b) The z-component of wind vector is zero on the sloped terrain.

(c) The wind vector is independent on x and y coordinates, and dependent only on z-coordinate.

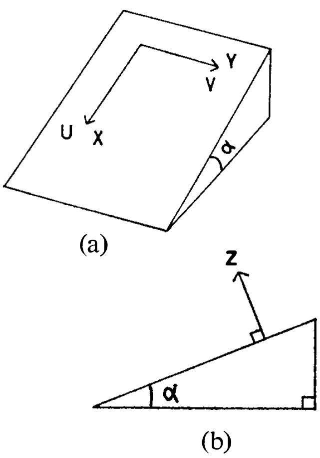

Fig 7 Coordinate system for governing equations

(d) Monin-Obukhov's similarity theory holds in each height of the Ekman layer.

(e) Local value of Monin-Obukhov length is defined by the heat and momentum flux of each height layer.

The present governing equations are the following;

$$O=\frac{d}{dz}\left(K\frac{du}{dz}\right)+f(v-v_g)+g\cdot\sin\alpha\cdot(\Theta-\theta)/\Theta\,, \tag{1}$$

$$O=\frac{d}{dz}\left(K\frac{dv}{dz}\right)-f(u-u_g)\,, \tag{2}$$

$$K=kz|\boldsymbol{\tau}/\rho|^{1/2}/\phi\,, \tag{3}$$

$$\phi=(1+12\,z/L)^{1/2}\,, \tag{4}$$

$$\boldsymbol{\tau}/\rho=K\frac{dV}{dz}\,, \tag{5}$$

$$q/C_p\rho=-K\frac{d\theta}{dz}\,, \tag{6}$$

$$z/L=k(g/\theta)(q/C_p\rho)z/|\boldsymbol{\tau}/\rho|^{3/2}\,, \tag{7}$$

$$V=u+iv\,, \tag{8}$$

$$V_g=u_g+iv_g\,, \tag{9}$$

$$\boldsymbol{\tau}=\tau_x+i\tau_y\,, \tag{10}$$

$$u_{gk}=u_g\,, \tag{11}$$

$$v_{gk}=v_g+v_k\,, \tag{12}$$

$$v_k=-(g/f)\cdot\sin\alpha\cdot(\Theta-\theta)/\Theta\,, \tag{13}$$

$$V_{gk}=u_{gk}+iv_{gk}\,, \tag{14}$$

$$|V|=\sqrt{u^2+v^2}\,, \tag{15}$$

$$|V_{gk}|=\sqrt{u_{gk}^2+v_{gk}^2}\,, \tag{16}$$

$$|\boldsymbol{\tau}|=\sqrt{\tau_x^2+\tau_y^2}\,, \tag{17}$$

$$i=\sqrt{-1}\,. \tag{18}$$

List of symbols

x : Along slope coordinate (see Fig 7 a),
y : Rectangular to x (see Fig 7 a),
z : Normal coordinate to x–y plane (see Fig. 7b),
u : Wind component (x-axis),

v : Wind component (y-axis),
K : Eddy diffusivity,
f : Coriolis parameter,
g : Gravity acceleration,
Θ : Upper layer potential temperature,
θ : Lower layer potential temperature,
α : Slope,
u_g : Geostrophic wind component (x-axis),
v_g : Geostrophic wind component (y-axis),
k : Von Kármán constant (k=0.41),
ϕ : Non-dimensional wind shear function,
L : Local value of Monin-Obukhov length,
$\boldsymbol{\tau}$: Shear stress vector,
ρ : Air density,
q : Heat flux,
C_p : Specific heat,
z_0 : Roughness length.

Eqs. (1) and (2) are the equations of motions. The third term of eq. (1) represents the effects of the ice slope. Eqs. (3) and (4) are the relation of eddy diffusivity and shear stress at each level. Eq. (4) is a non-dimensional wind shear function. Eq. (6) is the transfer equation of heat.

3.2. Non-dimensional wind shear function (ϕ)

The functions (ϕ) of the surface boundary layer were reported by a number of

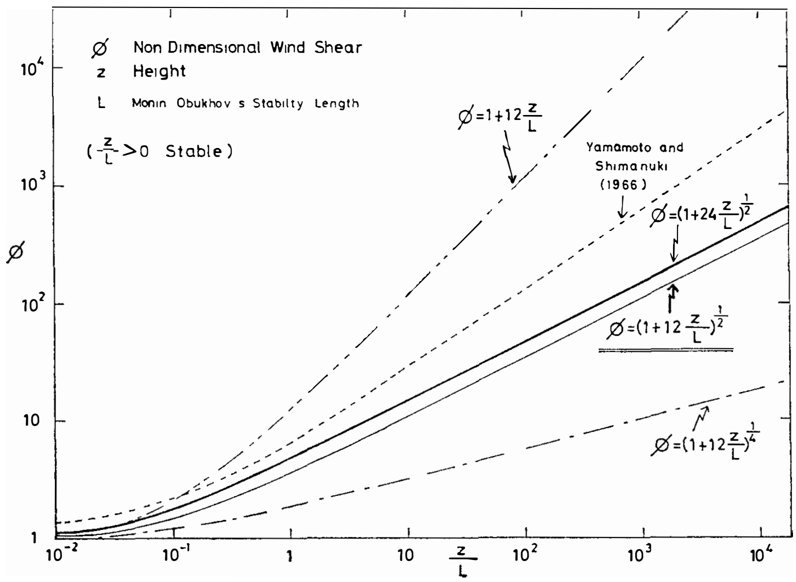

Fig 8 Example of non-dimensional wind shear functions.

researchers. However, the function, ϕ generally applicable to the Ekman layer was not found Fig. 8 shows some functions (ϕ) which were tested with numerical simulations of the wind velocity in the Ekman layer by ADACHI (1979). Then eq. (4) was found fit best for the neutral or stable Ekman layer.

In this paper the new function (ϕ: eq. (4)) is assumed in the stable Ekman layer at Syowa Station.

3.3. Boundary conditions and input data

Boundary conditions of this simulation model are as follows;

$$V=0, \text{ at } z=z_0$$

$$V=V_g \text{ and } \tau/\rho=0, \text{ at } z\to\infty$$

Input data of this simulation model are as follows;

(a) Potential temperature profile $\theta(z)$ Observed potential temperature profile is used in this model

(b) Geostrophic wind profile $V_g(z)$.

(c) The slope of the terrain (α).

The resultant geostrophic vector of the wind and the effect of the slope are assumed to have the following gradient and value (see $|V_{gk}|$ of Fig. 9).

$$\begin{cases} \dfrac{\partial v_{gk}}{\partial z}=\begin{cases} -2.5\ m/s/1000\ m, \text{ at } \underline{z\geq}1000\ m \\ -25\ m/s/1000\ m, \text{ at } 0<z<1000\ m\,, \end{cases} & (19) \\ u_{gk}=0\,. & (20) \end{cases}$$

3.4. Procedure of computation

The non-linear differential equations are solved by the combination of the approximation method and the relaxation method. This combination method was employed by ADACHI (1970)

4. Results of Computation and Comparison with Observation

Fig. 9a shows the calculated vertical profile of the resultant wind speed. The height of maximum wind speed is 150 m. This agrees with observed profile.

The computed wind spiral is shown in Fig 9b. This wind spiral is counterclockwise, same as the observed spiral.

According to Fig 9 b, the angle between the direction of the surface wind and that of the surface slope is 50 degrees On the other hand, the observed values of that angle are 29～50 degrees (see Figs 2c, 3c, 4c, 5c)

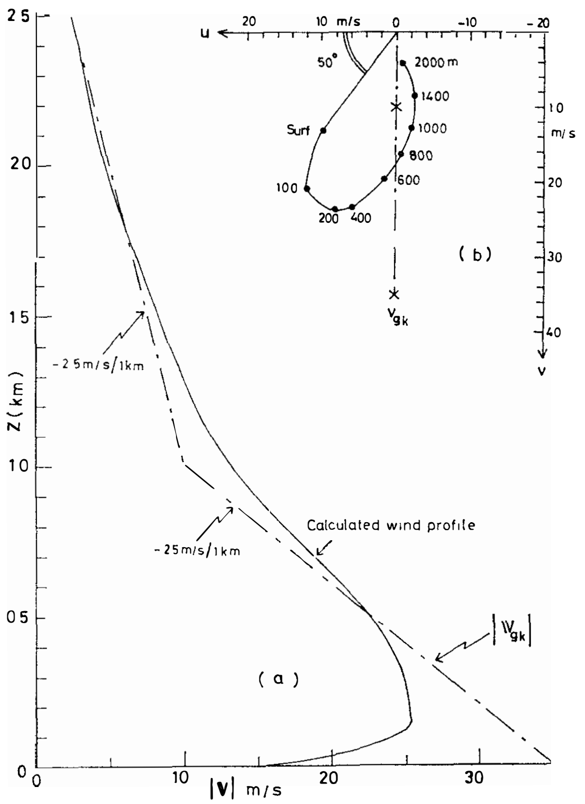

Fig. 9. Calculated wind profile (a) and wind spiral (b).

5. Concluding Remarks

The present numerical model successfully simulated the pattern of the strong katabatic wind profile.

But it is a future problem to find the real geostrophic wind and the real effect of the slope at Syowa Station.

Acknowledgments

The author is very grateful to Emeritus Prof. G. YAMAMOTO, Prof. J. KONDO and Dr. N. YASUDA*, Faculty of Science, Tohoku University, for their valuable advice and suggestions on this study.

The author would like to express his gratitude to Dr. S. OHTA, Director of Research Institute, Japan Weather Association, for his continuing encouragement, and to Dr. S. YOSHIDA, Japan Weather Association, and Associate Prof. O. CHIBA, Faculty of Science, Kochi University, for reading the manuscript and offering useful criticism.

* Present affiliation: Meteorological Research Institute, Tokyo

The author is grateful also to the staff of Antarctic Office, Japan Meteorological Agency, for supplying the meteorological data at Syowa Station.

References

ADACHI, T. (1970): Ekman spiral in baroclinic atmosphere Master's Thesis of Tohoku University.

ADACHI, T (1974): Nankyoku Syowa Kiti ni okeru ranryû kansoku (I) (Observation of atmospheric turbulence at Syowa Station in Antarctica (I)) Nankyoku Shiryô (Antarct Rec), **47**, 62–76.

ADACHI, T. (1979): Non-dimensional wind shear function applicable to neutral or stable baroclinic atmosphere in the planetary boundary layer private communication

BALL, F K (1956) The theory of strong katabatic winds Aust J Phys , **9**, 373–386.

BALL, F K (1960). Winds on the ice slopes of Antarctica Antarctic Meteorology. Oxford, Pergamon Press, 9–16.

JAPAN METEOROLOGICAL AGENCY (1971) Meteorological data at the Syowa Station in 1969. Antarct Meteorol Data, **10**, 147 p.

JAPAN METEOROLOGICAL AGENCY (1971) Meteorological data at the Syowa Station in 1970. Antarct Meteorol. Data, **11**, 151 p

JAPAN METEOROLOGICAL AGENCY (1973) Meteorological data at the Syowa Station in 1971. Antarct Meteorol Data, **12**, 149 p

KOBAYASHI, S. (1978): Vertical structure of katabatic winds in Mizuho Plateau Mem Natl Inst Polar Res , Spec Issue, **7**, 72–80.

LETTAU, H. H. (1966). A case study of katabatic flow on the south polar plateau Studies in Antarctic Meteorology. Washington, Am. Geophys Union, 1–11 (Antarct Res. Ser , **9**).

LYKOSOV, V. N and GUTMAN, L N (1972) Turbulent boundary layer above a sloping underling surface Izv. Acad. Sci USSR, Atmos Ocean. Phys , **8**, 799–809

MORITA, Y. (1968): Syowa Kiti de kansoku sareru katabatikku-fû ni tsuite (1) (Winds of katabatic origin observed at Syowa Station (1)). Nankyoku Shiryô (Antarct Rec), **31**, 21–32.

SHIMIZU, H., YOSHIMURA, I , NARUSE, R. and YOKOYAMA, K. (1978): Morphological feature of the ice sheet in Mizuho Plateau. Mem. Natl Inst Polar Res , Spec. Issue, **7**, 14–25.

YAMAMOTO, G., and SHIMANUKI, A (1966). Turbulent transfer in diabatic conditions. J Meteorol Soc. Jpn, **44**, 301–307.

(*Received March 16, 1979*)